Artvin Çoruh Üniversitesi
Doğal Afetler Uygulama ve Araştırma Merkezi
Doğal Afetler ve Çevre Dergisi

Artvin Çoruh University
Natural Hazards Application and Research Center
Journal of Natural Hazards and Environment

Araştırma Makalesi / Research Article, Doğ Afet Çev Derg, 2024; 10(2): 365-381, DOI: 10.21324/dacd.1422683

Analysing the Effects of Atmospheric Teleconnections on Streamflow Regime in the Eastern Black Sea Basin in Türkiye

Cenk Sezen[1,*]

[1]*Ondokız Mayıs University, Faculty of Engineering, Department of Civil Engineering, 55139, Samsun, Türkiye.*

Abstract

Analysing the variations in hydrological cycle components is essential for water resources planning and management. In this study, the relationship between the streamflow data belonging to five discharge gauging stations in the Eastern Black Sea Basin in Türkiye and the Arctic Oscillation (AO), East Atlantic-Western Russia (EAWR), North Atlantic Oscillation (NAO) and North Sea Caspian Pattern (NCP) was investigated. For this purpose, Spearman's correlation test, ensemble empirical mode decomposition (EEMD) and relative importance analysis were used. Accordingly, Spearman's correlation coefficients were calculated between raw streamflow data, decomposed streamflow data via EEMD and atmospheric teleconnections. Then, the relative importance analysis was applied to determine the atmospheric teleconnections' influences on streamflow data. The findings showed that the relationship between raw streamflow data and atmospheric teleconnections is generally more significant and negative in the winter and spring. Furthermore, it was observed that the linkage between the decomposed streamflow data and atmospheric teleconnections could differentiate. Although no significant correlation between atmospheric teleconnections and raw streamflow data was detected in some months, significant correlations were detected between atmospheric teleconnections and decomposed streamflow data. This reveals the importance of examining the relationship between atmospheric teleconnections and streamflow data for different periods. The relative importance analysis revealed that the influence of atmospheric teleconnections on streamflow data could change from station to station and from component to component. This study showed that investigating the effects of atmospheric teleconnections on streamflow data for different components and periods is important.

Keywords

Streamflow, Atmospheric Teleconnections, EEMD, Correlation, Relative Importance, Eastern Black Sea

Türkiye'nin Doğu Karadeniz Havzası'nda Atmosferik Tele Bağlantıların Akarsu Rejimi Üzerindeki Etkilerinin Analiz Edilmesi

Özet

Hidrolojik döngü bileşenlerindeki değişimlerin analiz edilmesi su kaynaklarının planlanması ve yönetilmesi açısından önem arz etmektedir. Bu çalışmada, Türkiye'nin Doğu Karadeniz Havzası'nda yer alan beş farklı akım gözlem istasyonuna ait akım verileri ile Arktik Salınım (AO), Doğu Atlantik-Batı Rusya Paterni (EAWR), Kuzey Atlantik Salınımı (NAO) ve Kuzey Denizi Hazar Paterni (NCP) arasındaki ilişki araştırılmıştır. Bu amaçla, Spearman's korelasyon testi, toplu ampirik mod ayrıştırma metodu (EEMD) ve nispi önem analizi kullanılmıştır. Buna göre, Spearman's korelasyon katsayıları hem ham akım verileri hem de EEMD ile bileşenlerine ayrılmış akım değerleri ile atmosferik tele bağlantılar arasında hesaplanmıştır. Daha sonra, atmosferik tele bağlantıların akım verileri üzerindeki etkisini belirlemek amacıyla nispi önem analizi uygulanmıştır. Elde edilen bulgular, ham akım verileri ile atmosferik tele bağlantılar arasındaki ilişkinin genel olarak kış ve ilkbahar aylarında daha önemli ve negatif olduğunu göstermiştir. Bununla birlikte, bileşenlerine ayrılmış akım verileri ile atmosferik tele bağlantılar arasındaki ilişkinin her bir bileşen için farklılık gösterebildiği gözlenmiştir. Atmosferik tele bağlantılar ile ham akım verileri arasında bazı aylar için herhangi bir ilişki bulunmamasına rağmen, bileşenlerine ayrılmış akım verileri ile atmosferik tele bağlantılar arasında önemli korelasyonlar tespit edilmiştir. Bu durum, atmosferik tele bağlantılar ile akım verileri arasındaki ilişkinin farklı periyotlarda incelenmesinin önemini ortaya koymaktadır. Nispi önem analizi atmosferik tele bağlantıların akım verileri üzerindeki etkisinin istasyondan istasyona ve bileşenden bileşene gösterdiğini ortaya koymuştur. Bu çalışma, atmosferik tele bağlantıların akım verileri üzerindeki etkisinin farklı bileşenler ve periyotlar için araştırılmasının önemini göstermiştir.

Anahtar Sözcükler

Akım, Atmosferik Tele Bağlantılar, EEMD, Korelasyon, Nispi Önem, Doğu Karadeniz

1. Introduction

Analysing the changes in hydrological cycle components are essential for water resources management. In addition, the effects of fluctuations in climatic parameters are essential for addressing extreme cases, such as floods and droughts.

* Sorumlu Yazar: Tel: +90 (362) 3121919 Faks: +90 (362) 3121919
E-posta: cenk.sezen@omu.edu.tr (Sezen C)

Gönderim Tarihi / Received : 19/01/2024
Kabul Tarihi / Accepted : 30/03/2024

The possible drivers behind the changes in hydrometeorological variables have been widely investigated (Oertel et al., 2020; Sharma et al., 2020; Gan et al., 2023). In these studies, the relationship between atmospheric teleconnections and different hydrometeorological variables has been put forward. Oertel et al. (2020) analysed the linkage between drought indices, namely Standardised Precipitation Evapotranspiration Index (SPEI) and Standardized Streamflow Index (SSI) and El Niño Southern Oscillation (ENSO) in central Chile. They revealed that ENSO could be efficient in dry periods in the summer and winter for SPEI-6 and SSI-6. Forootan et al. (2019) examined the linkage between hydrological droughts from 2003-2016 and atmospheric teleconnections, globally. They pointed out that the ENSO was influential in the greater parts of many continents, such as Asia and the Australian continent in different periods. They also stated that the Indian Ocean Dipole (IOD) and North Atlantic Oscillation (NAO) had regional effects on hydrological droughts. Sharma et al. (2020) investigated the impacts of the ENSO, IOD on the hydrometeorological extremes in the Tapi Basin, India. They revealed that positive IOD and weak El Niño conditions could be more efficient on higher flood risk in the basin. Zhang et al. (2020a) analysed the global variations of short-term concurrent hot and dry extremes (SCHDE) and their linkage with climate indices. They stated that the Pacific Decadal Oscillation (PDO)'s cold phases during the La Niña events could be a driver on the fortification of the SCHDE events in southern South America and Australia. Zhang et al. (2020b) scrutinized the tendencies in hydrometeorological variables in the Yarlung Zangbo River Basin in China and the potential relationship between trends and large-scale circulation. In some stations, they detected significant negative correlations between streamflow, temperature, precipitation, and the PDO, multivariate ENSO index (MEI). Gan et al. (2023) scrutinised the variations in hydrometeorological events (precipitation and drought) and analysed the effects of potential factors on the variations in the Huaihe River Basin, China. They revealed that the extreme precipitation and drought had significant and changeable characteristics across the basin. They also showed that the Arctic Oscillation (AO) was the most efficient index on the extreme hydrological index of the basin, and the Southern Oscillation Index (SOI) and NAO were influential on drought.

The linkage between hydrometeorological variables and atmospheric teleconnections in Türkiye has been analysed in many studies (Kutiel et al., 2002; Turkes & Erlat, 2003; Turkes & Erlat, 2008). Tosunoglu et al. (2018) examined the impacts of the NAO, SOI, North-Sea Caspian Pattern (NCP) on Standard Precipitation Index (SPI) in Türkiye. They found that the NAO was more efficient in the central and west Anatolia regions, whereas the NCP is more dominant in the eastern and northern regions. Duzenli et al. (2018) investigated the potential effects of atmospheric teleconnections, such as NAO, AO, SOI, and Western Mediterranean Oscillation (WMO), on the extreme precipitation variability in Türkiye. They found that the NAO is impactful on the extreme precipitation variability in the regions mostly affected by the Mediterranean climate, particularly in winter. Vazifehkhah and Kahya (2018) examined the influences of the NAO and AO extreme phases on hydrological drought, focusing on the standardised streamflow index (SSFI) in Türkiye and northern Iran. They found that NAO's and AO's negative extreme phases could lead to wetter conditions in the winter and spring in Türkiye, whereas the NAO and AO could be influential in Iran during only winter. Demir (2019) analysed the effects of the SOI on rainfall data of Central Anatolia, Turkey. Demir (2019) stated that La Nina could be influential in increasing precipitation, whereas El Nino could be efficient in decreasing precipitation. Yilmaz et al. (2020) investigated the relationship between NAO and precipitation in the Black Sea region. They found a negative, weak linkage between NAO and precipitation data. Abdelkader and Yerdelen (2022) scrutinised the linkage between the standardised streamflow index (SSFI) and atmospheric teleconnections, such as the ENSO, NAO, and Atlantic Multidecadal Oscillation (AMO) in Meriç Basin, Türkiye. They revealed that positive NAO and negative AMO phases could be related to the drought events. They also stated that the maximum dry conditions correspond to the La Nina events, whereas the maximum wet conditions coincide with the El Nino events. Akbas and Ozdemir (2023) investigated the impacts of atmospheric teleconnections on hydroclimatic variables (i.e., rainfall and runoff) using principal component analysis (PCA) and trend analysis approaches in the Marmara Sea River basins in Türkiye. They revealed that the NAO had high correlations with rainfall and runoff PC scores, especially in winter. Sezen (2023) analysed trends in streamflow using a wavelet-based approach (i.e., Innovative Polygon Trend Analysis (W-IPTA)) in the Konya Closed Basin, Türkiye. Significant short-term and long-term trends were found in the basin, and a significant negative relationship between the variability in streamflow and the NAO, AO, and NCP was obtained, particularly in winter. The implementation of data decomposition techniques has increased in recent years for analysing the trends in hydrometeorological variables and the effects of atmospheric teleconnections on the hydrometeorological variables (Abdelkader & Yerdelen, 2022; Sezen, 2023). In these studies, it was revealed that examining the changes in hydrometeorological variables using data decomposition techniques can be helpful for a periodical analysis. However, investigating the impacts of atmospheric teleconnections on hydrometeorological variables using the decomposition techniques has been comparatively less.

Analysing and determining the tendencies in hydrological components is substantial for efficient water resources management. Within this scope, using different approaches is significant to investigate the variability in hydrometeorological variables and the effects of atmospheric teleconnections on these variables.

In this study, the NAO, AO, NCP, and East Atlantic/Western Russia (EAWR) indexes' influence on the streamflow data in the Eastern Black Sea basin in Türkiye were investigated. First, Spearman's rank correlation analysis was used to analyse the linkage between streamflow data and related atmospheric teleconnections. Then, the Ensemble Empirical Mode Decomposition (EEMD) method was applied to streamflow data for the decomposition process. Thus, the linkage between streamflow data and atmospheric teleconnections was examined for different frequency components.

Finally, the relative importance of the atmospheric teleconnections regarding their effects on streamflow data was analysed. Investigating the potential impacts of atmospheric teleconnections by implementing the EEMD and relative importance analysis represents the novel aspects of this research.

2. Data and Methodology

2.1 Study area and data used

The linkage between streamflow data and atmospheric teleconnections was analysed in the Eastern Black Sea Basin situated in the north-eastern part of Türkiye (Figure 1). The Eastern Black Sea Basin generally has a regular precipitation regime, especially in the coastal parts, whereas dry weather conditions are dominant in the interior parts during summer. The geographical formations affect the precipitation regime across the basin. In this regard, the coastal parts have mild and wet conditions in winter and moderate and relatively wet during summer. On the other hand, interior parts have wet and cold climate conditions in winter and dry and hot climate characteristics in summer. The basin has significant water resources based on the precipitation characteristics, and rivers generally are not dry due to the redundant precipitation and snowmelt and relatively less evaporation in mild climate conditions (General Directorate of Water Management, 2020). The streamflow data from five discharge gauging stations was obtained from the General Directorate for State Hydraulic Works. The stations' spatial information and streamflow data statistics are given in Table 1 and Table 2, respectively. Accordingly, the data length changes from 35 to 36 years, and the altitude varies between 41 and 1296 m, as seen in Table 1. The annual mean streamflow is higher in the eastern regions than the western part, according to Table 2. The standard deviation and maximum values are also high in the eastern part of the basin.

Table 1: Location, data period and length of the discharge gauging stations

Station no	Station name	Location	Altitude (m)	Data period	Data length (years)
EİE 2202	Kara Dere-Değirmencik Köyü	40.007° E-40.85° N	78	1980-2015	36
EİE 2215	Çamlık Dere-Dereköy	40.6° E-40.73° N	942	1980-2014	35
EİE 2233	Tozköy Deresi-Tozköy	40.58° E-40.67° N	1296	1980-2015	36
EİE 2245	Terme Çayı-Gökçeli	36.83° E-41.08° N	66	1980-2015	36
EİE 2247	Melet Çayı-Gocallı Köprüsü	37.9° E-40.89° N	41	1980-2014	35

Table 2: Statistical data regarding annual streamflow data

		Statistics					
Station no	Station name	Minimum (m^3/s)	Mean (m^3/s)	Standard Deviation (m^3/s)	Maximum (m^3/s)	Skewness	Kurtosis
EİE 2202	Kara Dere-Değirmencik Köyü	6.34	10.99	2.02	15.89	0.20	0.76
EİE 2215	Çamlık Dere-Dereköy	10.13	13.68	1.83	17.24	0.02	-0.44
EİE 2233	Tozköy Deresi-Tozköy	4.75	6.66	1.04	8.62	0.07	-0.70
EİE 2245	Terme Çayı-Gökçeli	3.91	7.34	1.64	10.37	-0.15	-0.43
EİE 2247	Melet Çayı-Gocallı Köprüsü	3.26	27.15	8.9	43.75	-0.45	1.07

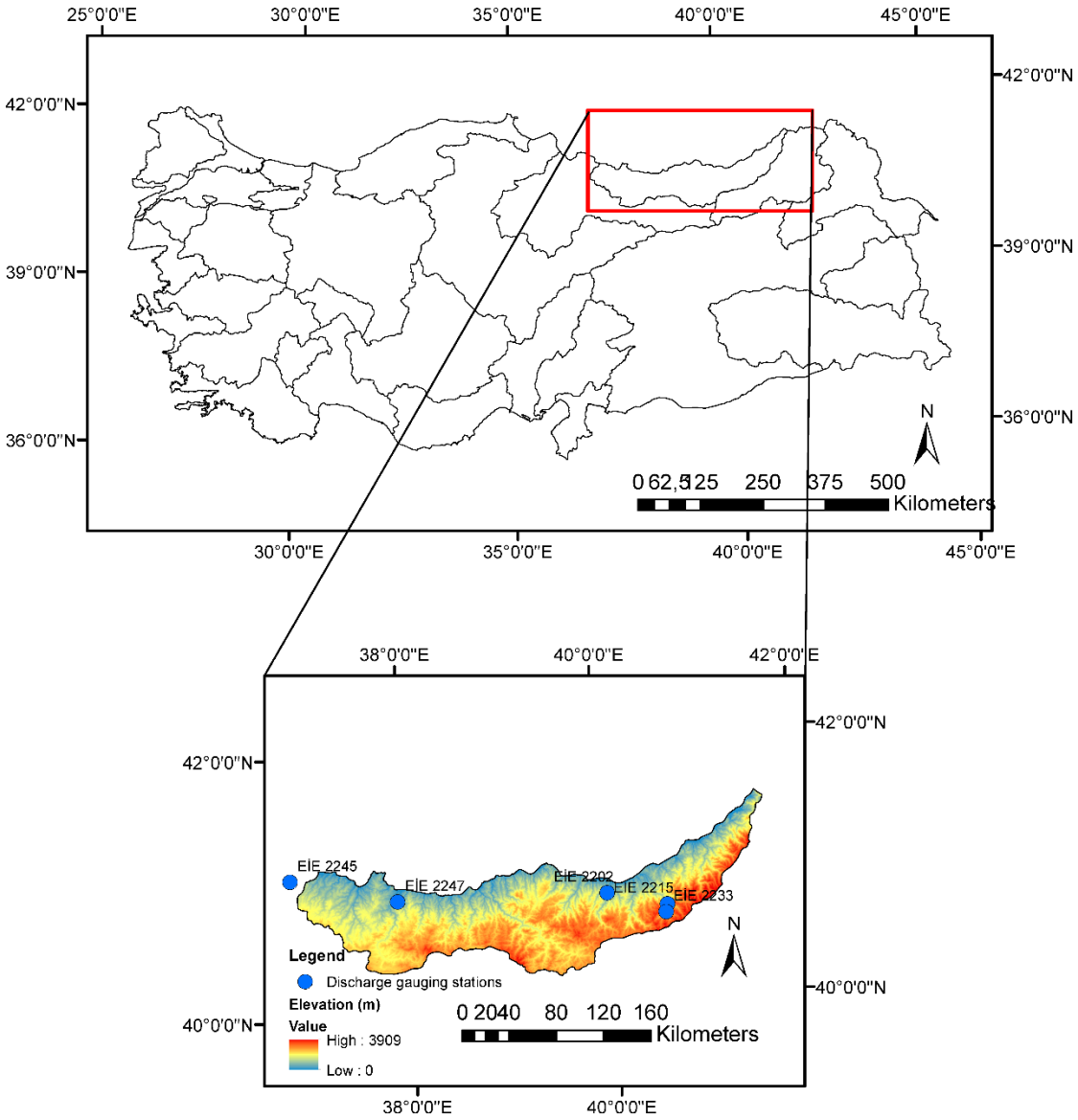

Figure 1: The study area's location and used discharge gauging stations. The blue circles refer to the discharge gauging stations

2.2 Atmospheric teleconnections

The NAO represents the variability of atmospheric mass between the subtropical Atlantic and Arctic, and changes in NAO's phases can lead to remarkable alterations in hydrometeorological parameters, such as surface temperature, winds, and precipitation in the Northern Hemisphere (Hurrell & Deser, 2010). The NAO's negative and positive phases can significantly affect changes in climatic variables. Turkes and Erlat (2003) revealed that precipitation tended to increase during the negative phase of the NAO (NAO (-)) for the winter and spring seasons and annually, while dry conditions were more dominant during the positive phase of the NAO in Türkiye. The AO is similar to the NAO; however, its main action centre envelops more of the Arctic, which gives the AO a more zonally symmetric view (Thompson & Wallace, 1998). The AO is an influential atmospheric teleconnection in the northern hemisphere. The negative and positive phases of the AO could trigger the variability in hydrometeorological variables. Turkes and Erlat (2008) pointed out that warmer signals dominate during the AO's negative phase, and cold signals are more influential during the AO' positive phase in Türkiye. The NCP is identified between the grids of the North Sea and northern Caspian by Kutiel and Benaroch (2002). The NCP's distinctive phases can significantly affect the changes in climatic parameters. Kutiel et al. (2002) found that temperature and precipitation had different tendencies under the NCP (-) and NCP (+) in the greater part of Türkiye. The EAWR is zonally oriented and has two principal anomaly centres across the Caspian Sea and Western Europe (Barnston & Livezey, 1987; Krichak & Alpert, 2005).

During the EAWR's negative phase, wetter conditions than typical weather characteristics were observed in most regions of the Mediterranean, whereas vice versa was obtained for the EAWR's positive phase (Barnston & Livezey, 1987; Krichak & Alpert, 2005). The NAO, AO, and EAWR data were obtained from the National Oceanic and Atmospheric Administration (NOAA) National Weather Service Climate Prediction Centre (NWS CPC) (https://www.cpc.ncep.noaa.gov). The NCP data were obtained from the University of East Anglia (UEA) Climatic Research Unit (CRU) (https://crudata.uea.ac.uk/cru/data/ncp/) and Sezen and Partal (2019).

2.3 Correlation analysis

Different correlation analysis approaches, such as Pearson's correlation and Spearman's rank correlation methods, have been generally used for investigating the effects of the atmospheric teleconnections on the hydrological variables. In this study, Spearman's rank correlation analysis was implemented since it has advantages, such as not having an assumption that both variables have a normal distribution. The Spearman's rank correlation coefficient formula is calculated as follows (Best & Roberts, 1975):

$$S = \sum_{i=1}^{n}(x_i - y_i)^2 \tag{1}$$

$$r_s = 1 - \frac{6S}{n(n^2-1)} \tag{2}$$

where, S stands for the difference between the two ranks of each variable (i.e., x_i and y_i), r_s stands for the Spearman's rank correlation coefficient, and n for the number of samples. Then, the significance of Spearman's rank correlation coefficients was evaluated according to the p values based on the AS89 algorithm (Best & Roberts, 1975).

2.4 Ensemble Empirical Mode Decomposition (EEMD)

The Ensemble Empirical Mode Decomposition (EEMD) is a time-space analysis technique which includes the white-noise-added data and an enhanced version of the Empirical Mode Decomposition (EMD) method (Wu & Huang, 2009). The EEMD is used for the original time series' decomposition in different modes which are called as finite intrinsic mode functions (IMFs) and a trend term (Wang et al., 2020). The steps for the EEMD analysis can be given as follows (Prasad et al., 2018; Wang et al., 2020):

1) Using the original time series (x(t)) and setting the EEMD parameters.
2) Adding a normally distributed white noise time series w(t) to x(t).

$$x'(t) = x(t) + w_i(t) \tag{3}$$

3) $x'(t)$ is decomposed into IMFs and trend or residue components.
4) The steps 2 and 3 are repeated for with various white noise series until the maximum ensemble number.
5) All IMF components' mean and residue components' mean avoiding the white noise are computed and time series can be obtained as follows:

$$x'(t) = \sum_{j=1}^{m} IMF_j + R_m \tag{4}$$

where, IMF_j represents the intrinsic mode functions, R_m denotes the residue component, and m is the total number of *IMFs*. The IMF_1 represents the highest frequency and maximum amplitude, whereas increasing IMFs refers to decreasing frequencies. In this study, the IMFs' number was obtained depending on the equation of m=$\log_2$(N)-1, where N stands for the time series' length (Guan, 2014). The empirical mode decomposition techniques were implemented in many hydrological modelling studies (Citakoglu & Coskun, 2022; Coskun & Citakoglu, 2023), and their usefulness was indicated in these studies.

2.5 Relative importance analysis

The relative importance of the atmospheric teleconnections regarding their effects on the streamflow regime was computed based on the R^2 partitioned by averaging over orders (Lindeman et al., 1980; Chevan & Sutherland, 1991). First, the linear regression equation was established between target data (i.e., streamflow data) and input data (i.e., AO, EAWR, NAO and NCP). The R^2 for a model with variables in regression in set S can be stated as follows (Gromping, 2006):

$$\hat{y}_i = c_0 + x_{i1}c_1 + \cdots + x_{ip}c_p$$

$$R^2(S) = \frac{Model\ SS(model\ with\ regressors\ in\ S)}{Total\ SS} = \frac{\sum_{i=1}^{n}(\hat{y}_i - \bar{y})^2}{\sum_{i=1}^{n}(y_i - \bar{y})^2} \quad (5)$$

where, $\hat{y}_i$ stands for the fitted response values, $\bar{y}$ for the mean of c for the predicted coefficients, and $x_{i1},\ldots,x_{ip}$ for input variables. R^2 quantifies the proportion of variation in the target variable (i.e., y) by considering regression input variables in the model. The additional R^2 in case of the addition of the regression variables in set M to a model with the regression input variables in set S can be expressed as follows:

$$seqR^2(M|S) = R^2(M \cup S) - R^2(S) \quad (6)$$

The order of the regression input data in any model is a permutation of the available regression input variables (i.e., $x_1,\ldots,x_p$) and can be referred to as the tuple of $r = (r_1,\ldots,r_p)$ indices. The portion of R^2 allocated to the regression variable x_k can be pointed out as follows:

$$seqR^2\big(\{x_k\}|S_k(r)\big) = R^2\big(\{x_k\} \cup S_k(r)\big) - R^2\big(S_k(r)\big) \quad (7)$$

where $S_k(r)$ stands for the regression variables entered into the model before the regression x_k in the order r (Gromping, 2006).

3. Results and Discussion

First, the correlation analysis between atmospheric teleconnections and raw streamflow data was fulfilled in Section 3.1. Then, the relationship between atmospheric teleconnections and decomposed streamflow data was presented in Section 3.2. The findings of the relative importance analysis were given to examine the influences of atmospheric teleconnections on streamflow data in Section 3.3. The analysis for investigating the relationship between atmospheric teleconnections and streamflow was carried out using Microsoft Excel (Microsoft Corperation, 2023), R programming language (R Core Team, 2023), and MATLAB Software (The MathWorks Inc., 2023). The flowchart regarding the adopted analysis is presented in Figure 2.

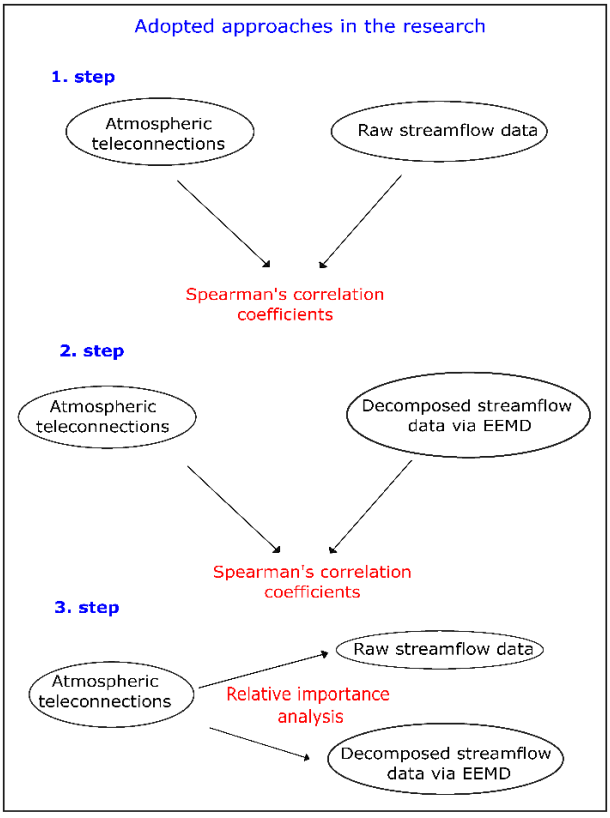

Figure 2: Adopted approaches for analyzing the relationship between atmospheric teleconnections and streamflow data

3.1 Correlation analysis results for raw streamflow data

First, the influences of the atmospheric teleconnections on raw streamflow data were investigated using the Spearman's correlation analysis. The correlations between the AO and streamflow data are not significant in all months, whereas significant positive correlations are observed between the NAO and streamflow in August in EİE 2202 (Figure 3). Furthermore, the EAWR and NCP are positively and significantly correlated with the streamflow regime, especially in the autumn. The highly negative correlations are observed between the AO and streamflow in February and March in EİE 2215 (Figure 4). The NAO and streamflow have a significant and negative linkage in EİE 2215, particularly in March and May. The EAWR has a significant negative relationship with streamflow data in February and April, and the significant negative correlations were observed between the NCP and streamflow in February, March, April, and May in EİE 2215. The NCP has a more significant relationship with the streamflow regime than other atmospheric teleconnections in EİE 2215. In EİE 2233, the relation between the NCP and raw streamflow data is highly negative and more significant in the winter and spring than other atmospheric teleconnections, according to Figure 5. There are no significant correlations between the AO, NAO and raw streamflow data in EİE 2233. Furthermore, a significant and negative correlation was obtained between the EAWR and streamflow data in April. The NCP has a significant and positive relationship with streamflow data in November and April, while any significant correlations were not obtained for other atmospheric teleconnections in EİE 2245 (Figure 6). In EİE 2247, significant and negative correlations were observed in February and April for the AO, and significant correlations were obtained in February and September, respectively for the NAO as seen in Figure 7. As for the EAWR and NCP, any significant correlations were not obtained in EİE 2247. The correlation analysis revealed that the effects of the atmospheric teleconnections on the streamflow data was similar to the findings of previous studies. Kebapcioglu and Partal (2021) showed that the correlations between the NAO, AO, and streamflow data were significant and negative correlations, in winter and annually in the Kızılırmak and Yeşilırmak basins, Türkiye. Furthermore, they detected that the AO and streamflow had a positive linkage in the autumn. Karabork et al. (2005) detected the significant effects of the NAO on precipitation and streamflow regimes in Türkiye in winter. Tosunoglu et al. (2018) obtained significant effects of the NAO on the Standard Precipitation Index (SPI) in the western and central parts of Türkiye, whereas NCP was more influential, especially in the northern and eastern parts of Türkiye. The NAO's, AO's, NCP's, and EAWR's influence on other meteorological variables were also detected in the region (Unal et al., 2012; Baltaci et al., 2018; Sezen & Partal, 2019). Unal et al. (2012) revealed a significant and negative linkage between the NCP and annual precipitation in the Eastern Black Sea region. Baltaci et al. (2018) pointed out that the EAWR was primarily positively correlated with precipitation anomalies in the Eastern Black Sea region and that positive EAWR could lead to wetter conditions. The positive relationship between the EAWR and raw streamflow data, especially in autumn, can be evaluated similarly to this finding. Sezen and Partal (2019) revealed a significantly negative linkage between the temperature and AO and NCP, whereas there is a positive relationship between the precipitation and related atmospheric teleconnections, particularly in the winter season. Similarly, the linkage between the raw streamflow and the NCP was mostly obtained positively, particularly in the autumn season in EİE 2202, EİE 2245 and EİE 2247. The AO and NAO have mostly negative correlations with the raw streamflow data in winter; however, they have a positive linkage with the raw streamflow, especially in the autumn months in EİE 2202, EİE 2245 and EİE 2247.

3.2 Correlation analysis results for decomposed streamflow data

The streamflow data of each station was decomposed into components using the EEMD analysis. In this respect, the four IMFs and one residual component belonging to the streamflow data were obtained based on the data length. Then, Spearman's correlation analysis was performed for each component. In EİE 2202, the AO and streamflow data have significantly positive linkage for IMF1 and residual components in October and August, respectively (Figure 3). The NAO and streamflow data have a significant positive linkage in the residual component in July and August, whereas the significant positive correlations were observed in high-frequency components (i.e., IMF2) in October and April in EİE 2202. The EAWR and streamflow data have significant positive correlations in high-frequency components in October, January, and February, while significant positive correlations in low-frequency components in November, March, and August in EİE 2202. In addition, significant negative correlations are also seen in February and August for IMF4 and IMF2 components, respectively. The NCP and streamflow data have significant positive and negative correlations for the IMF2 and IMF3 components in October and August, respectively.

In EİE 2215, the AO and streamflow have significant negative correlations, especially for IMF2, IMF3, and IMF4 in February, May and June (Figure 4). The NAO and streamflow have a significant negative and positive relation in spring and summer, respectively in EİE 2215. The NAO and streamflow have a positive relationship, particularly for IMF4 and residual components in July and August. The relationship between the EAWR and streamflow is significantly negative in February and April for IMF1 and in November and February for IMF4 in EİE 2215. The NCP and streamflow have a significant negative linkage for the high-frequency components, especially for IMF1 in February, March, April, and May. Significant correlations were not obtained for the low-frequency components between the NCP and streamflow.

In EİE 2233, significant positive correlations were observed in October for IMF2 and August for the residual component considering the AO's effect (Figure 5). Significant negative correlations were obtained in February for IMF2 and IMF3, whereas positive relationship was observed in August for the IMF4 and residual components between the NAO and streamflow. The EAWR and streamflow have negative correlations in the winter season, while they have positive correlations in October (for IMF1 and IMF3) and May and August (for the low-frequency components). The NCP and streamflow have negative correlations for the high-frequency components in March, April, and May, whereas they have positive correlations in the low-frequency components.

In EİE 2245, the AO's influence on the streamflow is negative in January, while the positive linkage was detected in May and July for high-frequency components, as seen in Figure 6. The NAO and streamflow have significant positive correlations in August and September. In addition, the NAO and streamflow has a significant and negative relationship in February (for IMF3), July and August (for the residual component). The EAWR and streamflow have a positive linkage in May and July and a negative relationship in January for the high-frequency components. The NCP and streamflow have a significant positive linkage in the autumn and spring.

In EİE 2247, the AO's effect on the streamflow is significantly positive and negative in the winter and summer, respectively, according to Figure 7. The NAO and streamflow have significant negative correlations, especially in February, and correlations are significantly negative and positive in the summer and autumn. The EAWR only had significant positive correlations for the high- and low-frequency components in August. Significant correlations were observed positively between the NCP and streamflow only in December and September.

The correlation analysis with EEMD revealed significant correlations for different components even though the raw streamflow data do not have any significant relationship with the atmospheric teleconnections. The correlations are primarily negative in winter and spring, while significant positive correlations were seen in summer and autumn. Furthermore, significant relationship is available for the high- and low-frequency components. This indicates that analysing the impacts of atmospheric teleconnections on hydrometeorological variables using decomposition techniques can be useful in revealing the complex linkage between the related variables. The advantages of using data decomposition techniques, such as wavelet analysis and EEMD, for the investigation of climatic variability were shown in previous studies (Rathinasamy et al., 2019; Wang et al., 2020; Shi et al., 2021). Wang et al. (2020) indicated the usefulness of the EEMD regarding the identification of more relevant and reasonable physical indices. Similarly, Wang et al. (2023) showed that wavelet analysis can help reveal the relationship between the hydrometeorological variables and atmospheric teleconnections. In this regard, implementing the data decomposition methods can be beneficial for comprehensively analysing the linkage between climatic variables and atmospheric teleconnections.

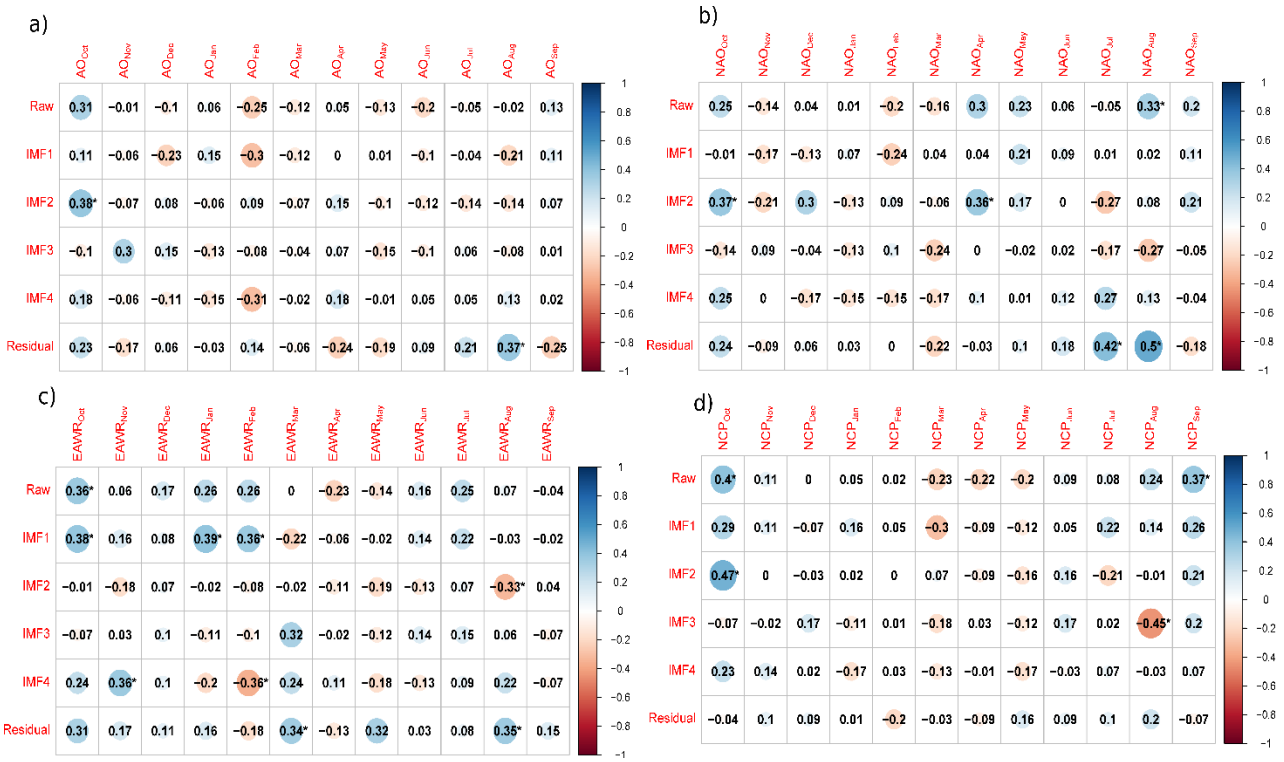

*Figure 3: Spearman's correlation coefficients between the raw and decomposed streamflow data and a) AO, b) NAO, c) EAWR, and d) NCP for EİE 2202. * term refers to the significant correlations at the significance level of α=0.05.*

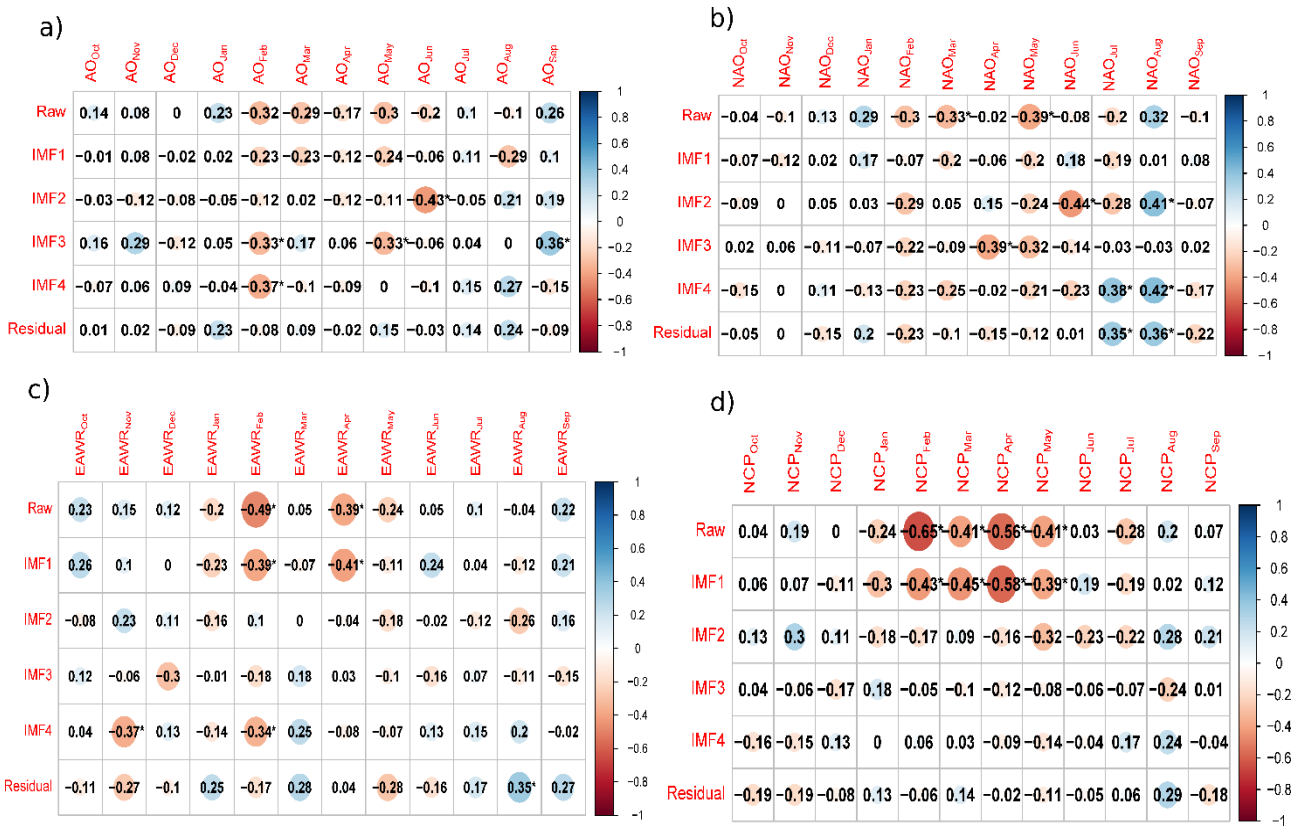

*Figure 4: Spearman's correlation coefficients between the raw and decomposed streamflow data and a) AO, b) NAO, c) EAWR, and d) NCP for EİE 2215. * term refers to the significant correlations at the significance level of α=0.05.*

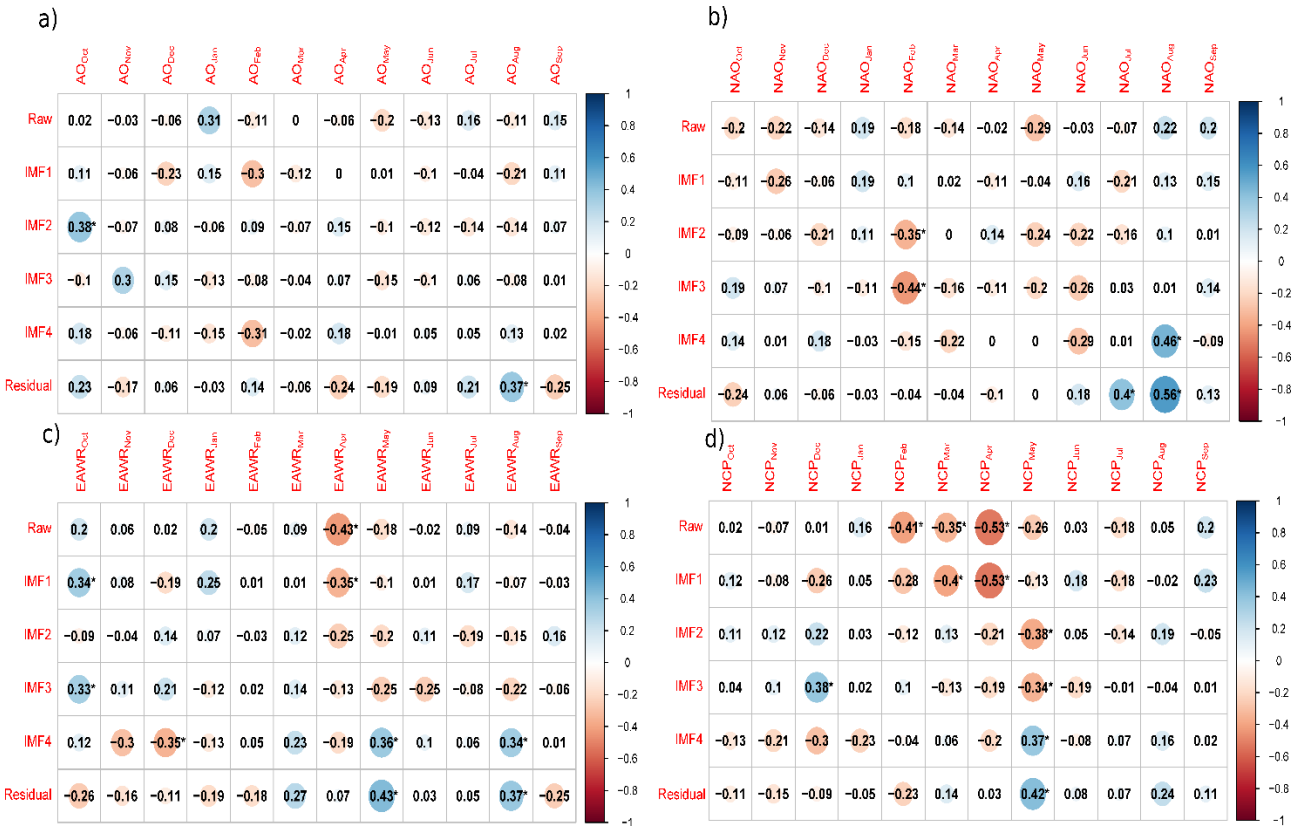

*Figure 5: Spearman's correlation coefficients between the raw and decomposed streamflow data and a) AO, b) NAO, c) EAWR, and d) NCP for EİE 2233. * term refers to the significant correlations at the significance level of α=0.05.*

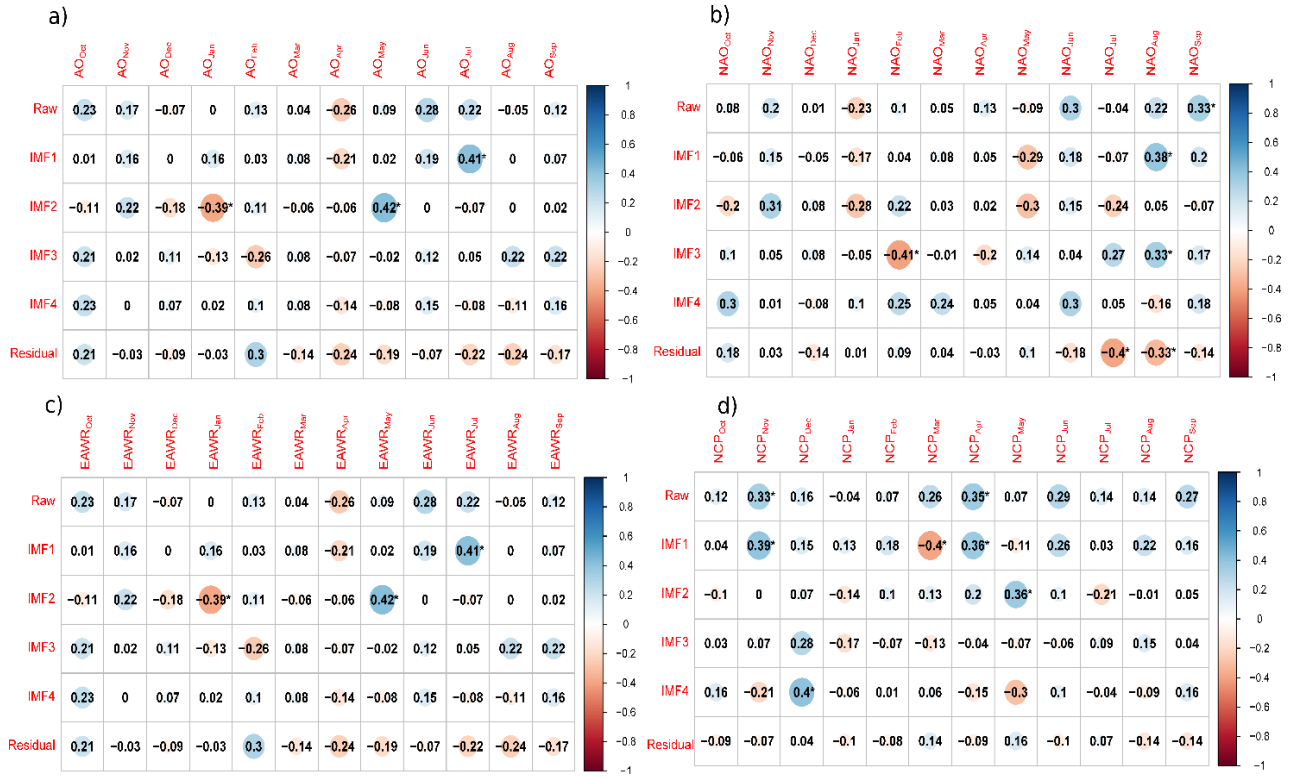

*Figure 6: Spearman's correlation coefficients between the raw and decomposed streamflow data and a) AO, b) NAO, c) EAWR, and d) NCP for EİE 2245. * term refers to the significant correlations at the significance level of α=0.05.*

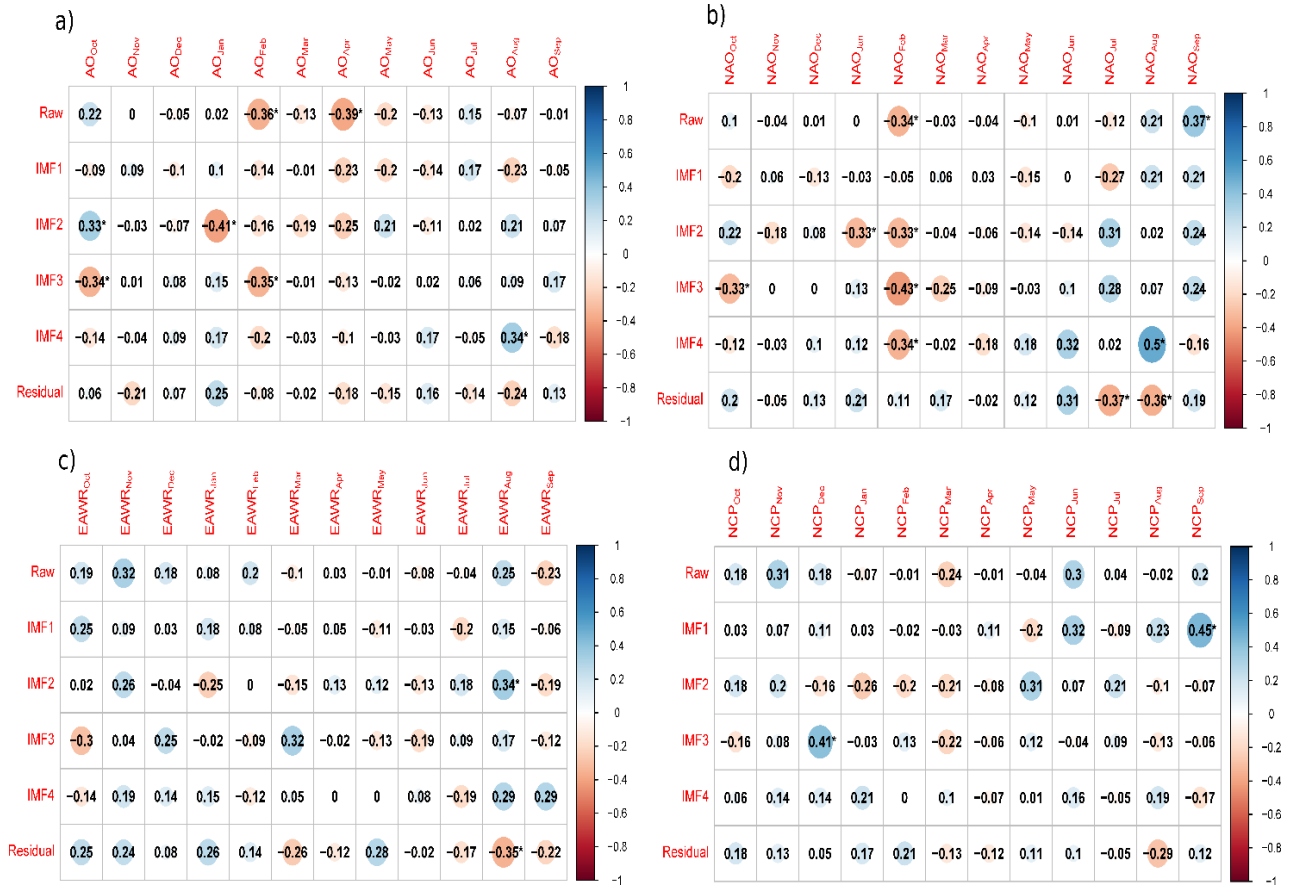

*Figure 7: Spearman's correlation coefficients between the raw and decomposed streamflow data and a) AO, b) NAO, c) EAWR, and d) NCP for EİE 2247. * term refers to the significant correlations at the significance level of α=0.05.*

3.3 Relative importance of the atmospheric teleconnections on the streamflow regime

In this section, the relative impact of the atmospheric teleconnections on the streamflow regime was scrutinized using the relative importance analysis. Accordingly, the importance of the atmospheric teleconnections, which can indicate their effects on the streamflow regime, was given as a rate for each station, as seen in Table 3, Table 4, Table 5, Table 6, and Table 7. As seen in Table 3, the relative importance of the NCP and EAWR is more than other atmospheric teleconnections' relative importance in the autumn and winter seasons, respectively, for EİE 2202. As for the IMF1 component, the NCP has more relative importance than other atmospheric teleconnections, especially in spring months, whereas the EAWR has more relative importance in winter. The NAO has remarkably high relative importance compared to AO, EAWR, and NCP in winter and spring for IMF2. The NAO, AO, and NCP have higher relative importance, particularly in winter, spring, and summer, respectively, for IMF3. The relative importance of the EAWR and NAO is generally over 50% in winter and summer, respectively, for IMF4. For the residual, the EAWR, AO and NAO have remarkable relative importance in winter, spring, and summer, respectively, in EİE 2202.

The relative importance of the atmospheric teleconnections related to their influence on the raw and decomposed streamflow data for EİE 2215 was presented in Table 4. Accordingly, the superior relative importance of the NCP is observed in winter and spring for raw streamflow data compared to other atmospheric teleconnections. Similarly, the NCP has higher relative importance rates in winter and spring than AO, EAWR, and NAO for IMF1, as seen in Table 4. Regarding IMF2, the EAWR and NAO have higher relative importance rates in winter and summer, respectively. The NCP has more remarkable relative importance rates than AO, EAWR, and NAO, particularly in autumn and spring for IMF2. The AO has higher relative importance rates in the spring and autumn seasons than EAWR, NAO and NCP for IMF3, while the relative importance of the EAWR is higher, particularly in summer. The NAO has more relative importance in spring and summer, whereas the EAWR has more relative importance rates in winter for IMF4. As for the residual component, it is observed that the relative importance of the EAWR is remarkably higher in winter and summer.

The atmospheric teleconnections' relative importance rates showing their relationship with streamflow data for EİE 2233 are given in Table 5. The NAO's relative importance is remarkably higher in the winter and autumn, while the effect of NCP is more dominant in spring for raw streamflow data. For IMF1, the NCP has higher relative importance rates in spring, while the AO has more influence in summer. The NAO has higher relative importance rates in autumn and winter, while the NCP has higher relative importance rates for IMF2. As for IMF3, the effect of the AO is more substantial in the autumn season, and the EAWR is more influential in the summer. The NAO's relative importance rate is higher in February and March and in summer for IMF4. The other atmospheric teleconnections also have high relative importance rates, which do not exhibit a seasonal tendency for IMF4. The EAWR has more influential rates than other atmospheric teleconnections in the winter and spring, whereas the NAO has more efficient relative importance rates for the residual component in summer.

The relationship between the streamflow data and the atmospheric teleconnections based on the relative importance analysis for EİE 2245 was presented in Table 6. It is observed that the EAWR has higher relative importance rates than the AO, NAO, and NCP, in winter and spring. The EAWR is efficient in December and January, whereas the NCP has higher relative importance in February and March for IMF1. As for IMF2, the AO has higher relative importance rates in winter, while the EAWR has higher relative importance rates in spring and summer. Furthermore, the NAO's relative importance rates are highly remarkable in autumn. The EAWR is dominant mainly in most months for IMF3, and higher relative importance rates of the EAWR are seen in winter and spring. The AO also has higher relative importance rates of over 70% in autumn for IMF3. The dominance of the EAWR is also evident for IMF4, particularly in autumn and winter. The NAO's relative importance rates are primarily high in the summer for IMF4. Regarding the residual component, the EAWR is more impactful in winter, while the NAO is more influential in summer.

The results showing the effects of the atmospheric teleconnection on streamflow data considering the relative importance analysis for EİE 2247 is shown in Table 7. The EAWR and NAO have higher relative importance rates for the raw streamflow data in autumn and winter, respectively. The EAWR and NAO are influential compared to AO and NCP in winter and spring, respectively, for IMF1. The NCP has remarkable relative importance rates, especially in winter and spring, whereas the EAWR has higher relative importance rates in summer for IMF2. As for IMF3, the NAO has higher relative importance rates in February, March, and summer. The AO and NAO have higher relative importance rates in spring and summer for IMF4. As for the residual component, the relative importance of the EAWR is substantially higher than the other atmospheric teleconnections' relative importance rates. Accordingly, it can be stated that the EAWR has remarkable relative importance rates in winter, spring, and summer for the residual component.

The relative importance analysis shows that the relative effect of each atmospheric teleconnection on the raw streamflow data and decomposed data for different periods can substantially change. In this regard, examining the impact of the atmospheric teleconnections on varied components is very important. Similar findings were emphasized in previous studies revealing the effects of atmospheric teleconnections on the hydrometeorological variables (Jiang et al., 2019; Sezen, 2023; Wang et al., 2023). All these studies indicated that the effects of atmospheric teleconnections on variables such as drought and streamflow can change for different periods. Accordingly, periodically investigating the influence of atmospheric teleconnections on hydrological components is substantial for water resources planning.

Furthermore, analysing the trends in hydrometeorological variables, using different methods, such as liner regression (LR), Man-Kendall (MK) analysis, and Spearman's Rho (SRHO) could give more comprehensive outlook to examine the changes and variations in hydrometeorological variables as indicated in previous studies (Yarbasi, 2019; Demir, 2019; Yilmaz et al., 2020; Citakoglu & Minarecioglu, 2021). Accordingly, investigating the relationship between the atmospheric teleconnections and hydrometeorological variables for different lags, analysing the trends in hydrometeorological variables for different periods and the linkage between the trends and atmospheric teleconnections, and using different decomposition techniques can pave the way for a broad perspective to enlarge the scope of this research. In this regard, in further studies, the variability in various hydrometeorological variables will be investigated using various trend analyses and further correlation analysis for different lags, and periodical analysis will be performed using different decomposition techniques such as wavelet transform.

Table 3: Relative importance rates for the EİE 2202 discharge gauging station.

		Months											
Streamflow data	**Atmospheric teleconnections**	**Oct**	**Nov**	**Dec**	**Jan**	**Feb**	**Mar**	**Apr**	**May**	**Jun**	**Jul**	**Aug**	**Sep**
Raw	AO	18%	16%	26%	3%	**31%**	5%	21%	25%	**57%**	23%	33%	3%
	EAWR	19%	7%	**54%**	**58%**	30%	14%	11%	2%	11%	**43%**	8%	1%
	NAO	8%	**70%**	7%	8%	21%	13%	**51%**	**51%**	25%	26%	**43%**	18%
	NCP	**55%**	7%	13%	31%	18%	**68%**	17%	22%	7%	8%	16%	**78%**
IMF1	AO	3%	6%	**69%**	3%	11%	11%	23%	10%	**59%**	27%	**50%**	9%
	EAWR	**59%**	20%	7%	**63%**	**69%**	4%	14%	2%	12%	18%	1%	2%
	NAO	4%	**55%**	20%	2%	6%	16%	26%	**68%**	25%	8%	8%	14%
	NCP	34%	19%	4%	32%	14%	**69%**	**37%**	20%	4%	**47%**	41%	**75%**
IMF2	AO	21%	6%	13%	7%	8%	8%	16%	25%	**40%**	13%	17%	9%
	EAWR	16%	26%	21%	23%	**70%**	**56%**	4%	16%	16%	19%	61%	1%
	NAO	13%	**58%**	**42%**	**40%**	10%	22%	**67%**	**40%**	14%	**43%**	19%	**52%**
	NCP	**50%**	10%	24%	30%	12%	14%	13%	19%	30%	25%	3%	38%
IMF3	AO	14%	**79%**	**40%**	25%	18%	16%	**38%**	**67%**	20%	9%	7%	6%
	EAWR	4%	2%	12%	13%	24%	**48%**	14%	3%	22%	15%	7%	29%
	NAO	**74%**	12%	26%	**47%**	**43%**	33%	23%	9%	13%	**67%**	17%	21%
	NCP	8%	7%	22%	15%	15%	3%	25%	21%	**45%**	9%	**69%**	**44%**
IMF4	AO	17%	7%	20%	16%	3%	9%	**41%**	3%	16%	7%	7%	2%
	EAWR	22%	**68%**	7%	**38%**	**63%**	**64%**	25%	46%	2%	20%	**79%**	17%
	NAO	**52%**	14%	**66%**	20%	10%	26%	2%	2%	**51%**	**60%**	11%	33%
	NCP	9%	11%	7%	26%	24%	1%	32%	**49%**	31%	13%	3%	**48%**
Residual	AO	22%	**63%**	14%	3%	7%	10%	**73%**	**41%**	12%	24%	16%	11%
	EAWR	24%	16%	**64%**	**48%**	**62%**	**66%**	16%	37%	18%	10%	35%	**67%**
	NAO	**39%**	17%	5%	11%	16%	19%	5%	18%	**49%**	**52%**	**40%**	18%
	NCP	15%	4%	17%	38%	15%	5%	6%	4%	21%	13%	9%	4%

Note: The bold rates show the highest relative importance rates for each month.

Table 4: Relative importance rates for the EİE 2215 discharge gauging station

		Months											
Streamflow data	**Atmospheric teleconnections**	**Oct**	**Nov**	**Dec**	**Jan**	**Feb**	**Mar**	**Apr**	**May**	**Jun**	**Jul**	**Aug**	**Sep**
Raw	AO	16%	27%	**60%**	8%	19%	6%	1%	6%	**59%**	25%	22%	**73%**
	EAWR	27%	6%	18%	31%	14%	8%	19%	8%	11%	20%	4%	13%
	NAO	**33%**	**44%**	15%	21%	24%	15%	1%	21%	15%	18%	**58%**	3%
	NCP	24%	23%	7%	**40%**	**42%**	**71%**	**79%**	**65%**	15%	**37%**	16%	11%
IMF1	AO	5%	33%	**52%**	4%	28%	8%	1%	3%	35%	**29%**	**80%**	10%
	EAWR	**63%**	7%	6%	20%	17%	0	22%	10%	10%	13%	2%	34%
	NAO	16%	**55%**	25%	20%	9%	6%	1%	3%	**37%**	**29%**	7%	**36%**
	NCP	16%	5%	17%	**56%**	**46%**	**86%**	**76%**	**84%**	18%	**29%**	11%	20%
IMF2	AO	6%	**43%**	12%	2%	11%	11%	28%	5%	**45%**	6%	24%	13%
	EAWR	22%	8%	**64%**	**70%**	23%	1%	7%	9%	10%	6%	33%	22%
	NAO	31%	8%	8%	2%	32%	33%	**43%**	20%	37%	**72%**	**36%**	13%
	NCP	**41%**	41%	16%	26%	**34%**	**55%**	22%	**66%**	8%	16%	7%	**52%**
IMF3	AO	**65%**	**77%**	4%	4%	17%	**41%**	16%	**72%**	7%	4%	2%	**53%**
	EAWR	12%	2%	**68%**	27%	**43%**	11%	1%	2%	**61%**	**47%**	0	36%
	NAO	14%	13%	3%	14%	26%	33%	**79%**	23%	18%	4%	43%	10%
	NCP	9%	8%	25%	**55%**	14%	15%	4%	3%	14%	45%	**55%**	1%
IMF4	AO	18%	8%	18%	16%	12%	11%	3%	21%	14%	22%	7%	9%
	EAWR	26%	**68%**	27%	**49%**	**57%**	41%	**47%**	10%	2%	34%	15%	3%
	NAO	24%	13%	**30%**	12%	7%	**45%**	24%	**54%**	**56%**	**35%**	**66%**	**79%**
	NCP	**32%**	11%	25%	23%	24%	3%	26%	15%	28%	9%	12%	9%
Residual	AO	**55%**	**49%**	23%	18%	9%	12%	29%	**39%**	26%	19%	11%	11%
	EAWR	3%	18%	4%	**53%**	**55%**	**55%**	7%	34%	3%	**33%**	**49%**	**49%**
	NAO	33%	10%	**68%**	9%	26%	25%	**57%**	23%	**43%**	30%	24%	19%
	NCP	9%	23%	5%	20%	10%	8%	7%	4%	28%	18%	16%	21%

Note: The bold rates show the highest relative importance rates for each month.

Table 5: Relative importance rates for the EİE 2233 discharge gauging station

		Months											
Streamflow data	**Atmospheric teleconnections**	**Oct**	**Nov**	**Dec**	**Jan**	**Feb**	**Mar**	**Apr**	**May**	**Jun**	**Jul**	**Aug**	**Sep**
Raw	AO	10%	19%	35%	**41%**	19%	13%	2%	3%	**52%**	**41%**	27%	25%
	EAWR	21%	2%	3%	30%	7%	18%	25%	9%	14%	15%	4%	1%
	NAO	**47%**	**75%**	**58%**	13%	**38%**	14%	1%	23%	15%	11%	**61%**	**38%**
	NCP	22%	4%	4%	16%	36%	**55%**	**72%**	**65%**	19%	33%	8%	36%
IMF1	AO	3%	14%	**45%**	2%	16%	2%	2%	4%	**41%**	**30%**	**47%**	5%
	EAWR	**62%**	8%	11%	**51%**	20%	1%	20%	19%	11%	25%	3%	1%
	NAO	13%	**72%**	10%	9%	6%	3%	3%	6%	31%	23%	40%	34%
	NCP	22%	6%	34%	38%	**58%**	**94%**	**75%**	**71%**	17%	22%	10%	**60%**
IMF2	AO	15%	41%	19%	**62%**	22%	3%	5%	3%	**39%**	5%	4%	1%
	EAWR	14%	4%	9%	10%	4%	11%	22%	13%	26%	36%	27%	**74%**
	NAO	**48%**	**44%**	**60%**	11%	**70%**	7%	**68%**	20%	19%	**50%**	9%	16%
	NCP	23%	11%	12%	17%	4%	**79%**	5%	**64%**	16%	9%	**60%**	9%
IMF3	AO	9%	**82%**	6%	18%	24%	37%	5%	8%	11%	11%	2%	**86%**
	EAWR	**54%**	2%	20%	**50%**	4%	8%	41%	**39%**	**58%**	21%	**69%**	5%
	NAO	26%	11%	5%	9%	**62%**	**41%**	1%	21%	21%	**52%**	23%	6%
	NCP	11%	5%	**69%**	23%	10%	14%	**53%**	32%	10%	16%	6%	3%
IMF4	AO	**47%**	18%	6%	23%	24%	11%	**54%**	1%	14%	**73%**	10%	3%
	EAWR	15%	**52%**	**45%**	18%	6%	42%	16%	42%	6%	11%	40%	30%
	NAO	17%	6%	25%	7%	**64%**	**43%**	8%	4%	**54%**	9%	**42%**	**57%**
	NCP	21%	24%	24%	**52%**	6%	4%	22%	**53%**	26%	7%	8%	10%
Residual	AO	11%	29%	11%	12%	21%	21%	19%	5%	14%	21%	15%	3%
	EAWR	24%	9%	**66%**	**60%**	21%	**53%**	26%	**52%**	10%	10%	31%	**75%**
	NAO	**57%**	6%	4%	5%	24%	18%	**50%**	2%	**52%**	**55%**	**45%**	5%
	NCP	8%	**56%**	19%	23%	**34%**	8%	5%	41%	24%	14%	9%	17%

Note: The bold rates show the highest relative importance rates for each month.

Table 6: Relative importance rates for the EİE 2245 discharge gauging station

		Months											
Streamflow data	**Atmospheric teleconnections**	**Oct**	**Nov**	**Dec**	**Jan**	**Feb**	**Mar**	**Apr**	**May**	**Jun**	**Jul**	**Aug**	**Sep**
Raw	AO	**48%**	8%	6%	10%	25%	5%	**45%**	18%	9%	26%	9%	14%
	EAWR	28%	21%	**67%**	**34%**	**54%**	**73%**	26%	**47%**	32%	**44%**	5%	6%
	NAO	16%	**36%**	3%	27%	8%	6%	5%	24%	18%	25%	**74%**	38%
	NCP	8%	35%	24%	29%	13%	16%	24%	11%	**41%**	5%	12%	**42%**
IMF1	AO	6%	8%	7%	24%	6%	3%	**36%**	17%	5%	**76%**	11%	4%
	EAWR	**74%**	21%	**45%**	**37%**	32%	42%	25%	23%	33%	9%	3%	3%
	NAO	10%	9%	23%	20%	8%	6%	7%	**52%**	9%	11%	**73%**	**73%**
	NCP	10%	**62%**	25%	19%	**54%**	**49%**	32%	8%	**53%**	4%	13%	20%
IMF2	AO	13%	9%	35%	**59%**	**43%**	17%	31%	23%	21%	7%	11%	11%
	EAWR	39%	15%	**38%**	7%	6%	**44%**	**35%**	6%	3%	**82%**	**54%**	16%
	NAO	**42%**	**70%**	18%	23%	33%	7%	5%	6%	**65%**	4%	4%	**42%**
	NCP	6%	6%	9%	11%	18%	32%	29%	**65%**	11%	7%	31%	31%
IMF3	AO	**75%**	33%	7%	4%	23%	12%	11%	3%	**49%**	9%	10%	**85%**
	EAWR	1%	**52%**	**58%**	**67%**	2%	**36%**	25%	**44%**	15%	24%	**50%**	7%
	NAO	18%	5%	4%	2%	**73%**	21%	26%	17%	22%	**54%**	34%	5%
	NCP	6%	10%	31%	27%	2%	31%	**38%**	36%	14%	13%	6%	3%
IMF4	AO	17%	18%	4%	14%	17%	11%	**31%**	3%	14%	**76%**	7%	9%
	EAWR	32%	**53%**	**58%**	**42%**	29%	**51%**	18%	37%	7%	5%	0	**61%**
	NAO	**43%**	6%	6%	4%	**47%**	32%	20%	11%	**54%**	10%	**75%**	6%
	NCP	8%	23%	32%	40%	7%	6%	31%	**49%**	25%	9%	18%	24%
Residual	AO	**34%**	17%	24%	8%	14%	17%	**76%**	35%	12%	20%	9%	8%
	EAWR	21%	20%	3%	**64%**	**52%**	**58%**	14%	**43%**	28%	9%	7%	**75%**
	NAO	27%	26%	**61%**	6%	4%	19%	4%	15%	**44%**	**56%**	**69%**	10%
	NCP	18%	**37%**	12%	22%	30%	6%	6%	7%	16%	15%	15%	7%

Note: The bold rates show the highest relative importance rates for each month.

Table 7: Relative importance rates for the EİE 2247 discharge gauging station

		Months											
Streamflow data	**Atmospheric teleconnections**	**Oct**	**Nov**	**Dec**	**Jan**	**Feb**	**Mar**	**Apr**	**May**	**Jun**	**Jul**	**Aug**	**Sep**
Raw	AO	25%	4%	10%	13%	19%	3%	**86%**	18%	32%	19%	30%	3%
	EAWR	**32%**	**57%**	**58%**	25%	29%	14%	4%	**49%**	19%	22%	**61%**	20%
	NAO	11%	18%	3%	**35%**	**40%**	3%	9%	28%	10%	**53%**	5%	**43%**
	NCP	**32%**	21%	29%	27%	12%	**80%**	1%	5%	**39%**	6%	4%	34%
IMF1	AO	6%	**58%**	**44%**	18%	22%	22%	**60%**	8%	27%	23%	**56%**	14%
	EAWR	**43%**	9%	8%	**43%**	**43%**	3%	8%	11%	13%	8%	16%	1%
	NAO	31%	19%	16%	10%	8%	**44%**	22%	**45%**	12%	**59%**	10%	13%
	NCP	20%	14%	32%	29%	27%	31%	10%	36%	**48%**	10%	18%	**72%**
IMF2	AO	**68%**	6%	5%	**43%**	14%	21%	18%	21%	18%	5%	6%	9%
	EAWR	3%	39%	23%	6%	14%	17%	**48%**	6%	**47%**	21%	**86%**	**43%**
	NAO	19%	**40%**	5%	42%	**36%**	7%	3%	22%	8%	**59%**	1%	17%
	NCP	10%	15%	**67%**	9%	**36%**	**55%**	31%	**51%**	**27%**	15%	7%	31%
IMF3	AO	**37%**	3%	5%	**69%**	20%	27%	**66%**	3%	19%	11%	2%	23%
	EAWR	28%	**82%**	21%	10%	6%	29%	2%	24%	9%	14%	**66%**	5%
	NAO	27%	2%	4%	14%	**62%**	**37%**	21%	2%	**43%**	**65%**	7%	**58%**
	NCP	8%	13%	**70%**	7%	12%	7%	11%	**71%**	29%	10%	25%	14%
IMF4	AO	**40%**	37%	17%	**35%**	19%	**64%**	**67%**	28%	24%	32%	9%	13%
	EAWR	22%	16%	**29%**	14%	21%	3%	3%	1%	30%	**54%**	34%	62%
	NAO	25%	5%	27%	28%	**51%**	33%	28%	**70%**	**33%**	10%	**48%**	6%
	NCP	13%	**42%**	27%	23%	9%	0	2%	1%	13%	4%	9%	19%
Residual	AO	17%	**55%**	6%	20%	19%	9%	**82%**	33%	18%	18%	12%	9%
	EAWR	19%	21%	**67%**	**51%**	19%	**56%**	7%	**42%**	27%	**32%**	**55%**	**55%**
	NAO	**58%**	20%	7%	10%	**40%**	27%	5%	20%	**38%**	31%	13%	14%
	NCP	6%	4%	20%	19%	22%	8%	6%	5%	17%	19%	20%	22%

Note: The bold rates show the highest relative importance rates for each month.

4. Conclusions

Analysing the variability and changes in hydrological components is critical for the efficient usage of water resources and for overcoming extreme phenomena. In this study, the relationship between the streamflow data and atmospheric teleconnections, namely AO, EAWR, NAO, and NCP, was analysed in the Eastern Black Sea Basin, Türkiye. In this respect, Spearman's rank correlation analysis, EEMD technique and relative importance analysis were implemented. According to the analysis results, the following findings were acquired:

- Significant correlations between raw streamflow data and atmospheric teleconnections were observed in the winter and spring. The significant correlations are mostly negative; however, positive correlations are also detected.
- The correlations between streamflow decomposed components and atmospheric teleconnections change for each component. Significant correlations between decomposed streamflow data and atmospheric teleconnections were observed in some cases, even though the raw streamflow data and atmospheric teleconnections did not have significant correlations. This shows that investigating the linkage between hydrometeorological data and atmospheric teleconnections for different periods is essential.
- The relative importance analysis reveals that the relative effect of each atmospheric teleconnection on the raw streamflow data and decomposed data for different periods can significantly alter.

This study shows that examining the effects of atmospheric teleconnections on streamflow data having different components and investigating their relative importance is significant regarding having a comprehensive outlook for investigating the variability in hydrometeorological variables. However, examining the relationship between the atmospheric teleconnections and hydrometeorological variables for several lags, analysing the trends in hydrometeorological variables for different periods, and implementing different data-decomposition approaches can remarkably improve the scope of this research topic and offering a distinctive outlook on this topic. In this respect, to improve the scope of this research, in further studies, an elaborate periodical analysis using different decomposition techniques, trend analysis methods, and correlation analysis for different lags will be used in various hydrometeorological variables.

Acknowledgement

The author offers his gratitude to the Turkish General Directorate of State Hydraulic Works for accessing the streamflow data.

References

Abdelkader, M., & Yerdelen, C. (2022). Hydrological drought variability and its teleconnections with climate indices. *Journal of Hydrology, 605*, Article 127290. https://doi.org/10.1016/j.jhydrol.2021.127290

Akbas, A., & Ozdemir, H. (2023). Influence of atmospheric circulation on the variability of hydroclimatic parameters in the Marmara Sea river basins. *Hydrological Sciences Journal, 68*(9), 1229-1240. https://doi.org/10.1080/02626667.2023.2206970

Baltaci, H., Akkoyunlu, B. O., & Tayanc, M. (2018). Relationships between teleconnection patterns and Turkish climatic extremes. *Theoretical and Applied Climatology, 134*, 1365-1386. https://doi.org/10.1007/s00704-017-2350-z

Barnston, A. G., & Livezey, R. E. (1987). Classification, seasonality and persistence of low-frequency atmospheric circulation patterns. *Monthly Weather Review, 115*(6), 1083-1126. https://doi.org/10.1175/1520-0493(1987)115<1083:CSAPOL>2.0.CO;2

Best, D. J., & Roberts, D. E. (1975). Algorithm AS 89: the upper tail probabilities of Spearman's rho. *Journal of the Royal Statistical Society. Series C (Applied Statistics), 24*(3), 377-379. https://doi.org/10.2307/2347111

Chevan, A., & Sutherland, M. (1991). Hierarchical partitioning. *The American Statistician, 45*(2), 90-96. https://doi.org/10.1080/00031305.1991.10475776

Citakoglu, H., & Minarecioglu, N. (2021). Trend analysis and change point determination for hydro-meteorological and groundwater data of Kizilirmak basin. *Theoretical and Applied Climatology, 145*(3), 1275-1292. https://doi.org/10.1007/s00704-021-03696-9

Citakoglu, H., & Coskun, O. (2022). Comparison of hybrid machine learning methods for the prediction of short-term meteorological droughts of Sakarya Meteorological Station in Turkey. *Environmental Science and Pollution Research, 29*(50), 75487-75511. https://doi.org/10.1007/s11356-022-21083-3

Coskun, O., & Citakoglu, H. (2023). Prediction of the standardized precipitation index based on the long short-term memory and empirical mode decomposition-extreme learning machine models: The Case of Sakarya, Türkiye. *Physics and Chemistry of the Earth, Parts A/B/C, 131*, Article 103418. https://doi.org/10.1016/j.pce.2023.103418

Demir, H. B. (2019). *Güneyli salınımın İç Anadolu Bölgesi yıllık yağış verileri üzerine etkisi* [Yüksek Lisans tezi, Konya Teknik Üniversitesi]. YÖK Ulusal Tez Merkezi. https://tez.yok.gov.tr/UlusalTezMerkezi

Duzenli, E., Tabari, H., Willems, P., & Yilmaz, M.T. (2018). Decadal variability analysis of extreme precipitation in Turkey and its relationship with teleconnection patterns. *Hydrological Processes, 32*(23), 3513-3528. https://doi.org/10.1002/hyp.13275

Kebapcioglu, E., & Partal, T. (2021). Yeşilırmak ve Kızılırmak Havzaları Akımları Üzerinde Kuzey Atlantik Salınımı ve Arktik Salınımının Etkilerinin Belirlenmesi. *DSI Technical Bulletin, 138*, 27-35.

Forootan, E., Khaki, M., Schumacher, M., Wulfmeyer, V., Mehrnegar, N., van Dijk, A. I., Brocca, L., Farzaneh, S., Akinluyi, F., Ramillien, G., Shum, C.K., Awange, J., & Mostafaie, A. (2019). Understanding the global hydrological droughts of 2003–2016 and their relationships with teleconnections. *Science of the Total Environment, 650*, 2587-2604. https://doi.org/10.1016/j.scitotenv.2018.09.231

Gan, R., Li, D., Chen, C., Yang, F., Zhang, X., & Guo, X. (2023). Spatiotemporal characteristics of extreme hydrometeorological events and its potential influencing factors in the Huaihe River Basin, China. *Stochastic Environmental Research and Risk Assessment, 37*, 2693–2712. https://doi.org/10.1007/s00477-023-02413-4

General Directorate of Water Management. (2020). *Flood Management Plans*. Retrieved July 17, 2023, from https://www.tarimorman.gov.tr/SYGM/Sayfalar/Detay.aspx?SayfaId=53

Gromping, U. (2006). Relative importance for linear regression in R: the package relaimpo. *Journal of Statistical Software, 17*, 1-27. https://doi.org/ 10.18637/jss.v017.i01

Guan, B.T. (2014). Ensemble empirical mode decomposition for analyzing phenological responses to warming. *Agricultural and Forest Meteorology, 194*, 1-7. https://doi.org/10.1016/j.agrformet.2014.03.010

Hurrell, J. W., & Deser, C. (2010). North Atlantic climate variability: the role of the North Atlantic Oscillation. *Journal of Marine Systems, 79*(3-4), 231-244. https://doi.org/10.1016/j.jmarsys.2009.11.002

Jiang, R., Wang, Y., Xie, J., Zhao, Y., Li, F., & Wang, X. (2019). Multiscale characteristics of Jing-Jin-Ji's seasonal precipitation and their teleconnection with large-scale climate indices. *Theoretical and Applied Climatology, 137*, 1495-1513. https://doi.org/10.1007/s00704-018-2682-3

Karabork, M. Ç., Kahya, E., & Karaca, M. (2005). The influences of the Southern and North Atlantic Oscillations on climatic surface variables in Turkey. *Hydrological Processes, 19*(6), 1185-1211. https://doi.org/10.1002/hyp.5560

Krichak, S. O., & Alpert, P. (2005). Decadal trends in the east Atlantic–west Russia pattern and Mediterranean precipitation. *International Journal of Climatology, 25*(2), 183-192. https://doi.org/10.1002/joc.1124

Kutiel, H., & Benaroch, Y. (2002). North Sea-Caspian Pattern (NCP)–an upper level atmospheric teleconnection affecting the Eastern Mediterranean: Identification and definition. *Theoretical and Applied Climatology, 71*, 17-28. https://doi.org/10.1007/s704-002-8205-x

Kutiel, H., Maheras, P., Turkes, M., & Paz, S. (2002). North Sea–Caspian Pattern (NCP)–an upper level atmospheric teleconnection affecting the eastern Mediterranean–implications on the regional climate. *Theoretical and Applied Climatology, 72*, 173-192. https://doi.org/10.1007/s00704-002-0674-8

Lindeman, R. H., Merenda, P. F., & Gold, R. Z. (1980). Introduction to bivariate and multivariate analysis. Scott, Foresman, Glenview, IL.

Microsoft Corporation. (2023). *Microsoft Excel*. https://office.microsoft.com/excel

Oertel, M., Meza, F.J., & Gironas, J. (2020). Observed trends and relationships between ENSO and standardized hydrometeorological drought indices in central Chile. *Hydrological Processes, 34*(2), 159-174. https://doi.org/10.1002/hyp.13596

Prasad, R., Deo, R.C., Li, Y., & Maraseni, T. (2018). Soil moisture forecasting by a hybrid machine learning technique: ELM integrated with ensemble empirical mode decomposition. *Geoderma, 330*, 136-161. https://doi.org/10.1016/j.geoderma.2018.05.035

R Core Team. (2023). *R: A language and environment for statistical computing*. R Foundation for Statistical Computing, Vienna, Austria. https://www.R-project.org/.

Rathinasamy, M., Agarwal, A., Sivakumar, B., Marwan, N., & Kurths, J. (2019). Wavelet analysis of precipitation extremes over India and teleconnections to climate indices. *Stochastic Environmental Research and Risk Assessment, 33*, 2053-2069. https://doi.org/10.1007/s00477-019-01738-3

Sezen, C., & Partal, T. (2019). The impacts of Arctic oscillation and the North Sea Caspian pattern on the temperature and precipitation regime in Turkey. *Meteorology and Atmospheric Physics, 131*, 1677-1696. https://doi.org/10.1007/s00703-019-00665-w

Sezen, C. (2023). A new wavelet combined innovative polygon trend analysis (W-IPTA) approach for investigating the trends in the streamflow regime in the Konya Closed Basin, Turkey. *Theoretical and Applied Climatology, 151*(3-4), 1523-1565. https://doi.org/10.1007/s00704-022-04328-6

Sharma, P. J., Patel, P. L., & Jothiprakash, V. (2020). Hydroclimatic teleconnections of large-scale oceanic-atmospheric circulations on hydrometeorological extremes of Tapi Basin, India. *Atmospheric Research, 235*, Article 104791. https://doi.org/10.1016/j.atmosres.2019.104791

Shi, X., Huang, Q., & Li, K. (2021). Decomposition-based teleconnection between monthly streamflow and global climatic oscillation. *Journal of Hydrology, 602*, Article 126651. https://doi.org/10.1016/j.jhydrol.2021.126651

The MathWorks Inc. (2023). *Natick, Massachusetts: The MathWorks Inc*. https://www.mathworks.com

Thompson, D. W., & Wallace, J. M. (1998). The Arctic Oscillation signature in the wintertime geopotential height and temperature fields. *Geophysical Research Letters, 25*(9), 1297-1300. https://doi.org/10.1029/98GL00950

Tosunoglu, F., Can, I., & Kahya, E. (2018). Evaluation of spatial and temporal relationships between large-scale atmospheric oscillations and meteorological drought indexes in Turkey. *International Journal of Climatology, 38*(12), 4579-4596. https://doi.org/10.1002/joc.5698

Turkes, M., & Erlat, E. (2003). Precipitation changes and variability in Turkey linked to the North Atlantic Oscillation during the period 1930–2000. *International Journal of Climatology, 23*(14), 1771-1796. https://doi.org/10.1002/joc.962

Turkes, M., & Erlat, E. (2008). Influence of the Arctic Oscillation on the variability of winter mean temperatures in Turkey. *Theoretical and Applied Climatology, 92*, 75-85. https://doi.org/10.1007/s00704-007-0310-8

Unal, Y. S., Deniz, A., Toros, H., & Incecik, S. (2012). Temporal and spatial patterns of precipitation variability for annual, wet, and dry seasons in Turkey. *International Journal of Climatology, 32*(3), 392-405. https://doi.org/10.1002/joc.2274

Vazifehkhah, S., & Kahya, E. (2018). Hydrological drought associations with extreme phases of the North Atlantic and Arctic Oscillations over Turkey and northern Iran. *International Journal of Climatology, 38*(12), 4459-4475. https://doi.org/10.1002/joc.5680

Wang, J., Wang, X., hui Lei, X., Wang, H., hua Zhang, X., jun You, J., feng Tan, Q., & lia Liu, X. (2020). Teleconnection analysis of monthly streamflow using ensemble empirical mode decomposition. *Journal of Hydrology, 582*, Article 124411. https://doi.org/10.1016/j.jhydrol.2019.124411

Wang, T., Song, C., & Chen, X. (2023). Clarifying the relationship between annual maximum daily precipitation and climate variables by wavelet analysis. *Atmospheric Research, 295*, Article 106981. https://doi.org/10.1016/j.atmosres.2023.106981

Wu, Z., & Huang, N. E. (2009). Ensemble empirical mode decomposition: a noise-assisted data analysis method. *Advances in Adaptive Data Analysis, 1*(1), 1-41. https://doi.org/10.1142/S1793536909000047

Yarbasi, G. E. (2019). *Güneyli salınımın Karadeniz Bölgesi yıllık yağış verileri üzerine etkisi* [Yüksek Lisans tezi, Konya Teknik Üniversitesi]. YÖK Ulusal Tez Merkezi. https://tez.yok.gov.tr/UlusalTezMerkezi

Yilmaz, C. B., Demir, V., & Sevimli, M. F. (2020). Karadeniz yağışlarının Kuzey Atlantik salınımı ile ilişkisi. *Gazi Mühendislik Bilimleri Dergisi, 6*(3), 248-254. https://dergipark.org.tr/en/pub/gmbd/issue/58697/772005

Zhang, H., Wu, C., Yeh, P. J. F., & Hu, B. X. (2020a). Global pattern of short-term concurrent hot and dry extremes and its relationship to large-scale climate indices. *International Journal of Climatology, 40*(14), 5906-5924. https://doi.org/10.1002/joc.6555

Zhang, R., Xu, Z., Zuo, D., & Ban, C. (2020b). Hydro-meteorological trends in the Yarlung Zangbo River Basin and possible associations with large-scale circulation. *Water, 12*(1), Article 144. https://doi.org/10.3390/w12010144